Optimizing Stresses in Cold Metal Transfer Welded 316L Austenitic Stainless Steel

Dipali Bhoyar[1] and Nischal Mungle[2]

[1]*Research Scholar PGTD Computer Science and Electronics, RTMNU, India*
[2]*Department of Mechanical Engineering, Yeshwantrao Chavan College of Engineering, Nagpur, India*
Email: bhoyar.dipali@gmail.com

Abstract: In the present study, the weld joints of Cold Metal Transfer (CMT) 316L ASS weld were investigated with three different heat inputs. The tensile strength of LHI welds (610 MPa) is the highest compared to MHI (603 MPa) and HHI (601 MPa) welds, which is due to the higher chromium and nickel content in the weld metal. The experimental findings were compared with the simulation outcomes using ANSYS R18.1. It was found that the total deformation of HHI welds was higher than that of MHI and LHI due to the content of alloying elements in the welds. The Von Misses stresses of LHI weld was found to be greater than MHI and HHI weld due to the input parameters during welding. The experimental results of yield strength are found to be lower than simulation which is helpful to predict the yielding criteria of ductile materials.

Keywords: Austenitic Stainless Steel, Cold Metal Transfer, Mechanical Properties, ANSYS.

1. Introduction

Materials studies for nuclear energy focuses on 316L austenitic stainless steel (ASS) due to its corrosion resistance and high-temperature mechanical properties [1]. Every year, the demand for stainless steel (SS) is increasing by an astonishing 5% [2-4]. Global production in 2019 exceeded 52 million tons. SS is currently adopted by a variety of industries [5]. As it is relatively expensive, but its extraordinary properties lead to extended service life and reduced costs. Currently, the industry has a growing trend of arranging higher performance processes and materials that help to drive economic growth [6]. Furthermore, achieving desirable mechanical properties and corrosion resistance essential for commercial sectors consisting of the pipelines in desalination plants, nuclear industry, and offshore pipelines (gas and oil), can be promoted by careful selection of welding materials [7]. With an extraordinary combination of higher strength, weldability, durability, ductility and corrosion resistance, the ASS is still the most commonly used grade [8-9]. Thermal cracks during the welding process reduce the weldability of the ASS [10]. Different optimization techniques are used to optimize the mechanical properties (tensile strength, yield strength, elongation (%)) of the welded joint. Haq et al. [11] conducted an experimental study using an L18 design, testing two distinct strain rates across various temperatures ranging from 750 °C to 900 °C in 75 °C intervals. Their findings revealed that as the temperature increased, the strain rate also increased, while the strength decreased. Dharavath et al. [12] studied 316L ASS to determine the forming limit diagram (FLM) under hot forming conditions and found that the modified Zerilli-Armstrong model (m-ZA) had better predictability of yield stress. Additionally, the researchers used simulation techniques, including the computer code ABAQUS 6.13, to predict formability between 750°C and 900°C. Mani et al. [13], used regression analysis to develop a mathematical model of the process characteristics and optimized different filler wire parameters (ultimate tensile strength and elongation) using a Non-dominated Sorting Genetic algorithm (NSGA II). Ghumman et al. [14], investigated the effects of welding parameters on surface roughness, hardness, and tensile strength during tungsten inert gas (TIG) welding of 316L ASS. The study aimed to understand how variations in welding parameters affect the quality of the welded joints in terms of surface finish, material hardness, and mechanical strength. They utilized an orthogonal Taguchi L9 array to determine the optimum values for tensile strength, microhardness, and surface roughness in the welding process. In the present study, 316L ASS welded with Cold Metal Transfer (CMT) using 316L

filler with three heat inputs. Experimental tests were conducted to examine the microstructure and mechanical properties and compared with simulation results obtained using ANSYS R18.1.This study revealed possible reasons for the significant mechanical properties compared with simulation results in the welded joints with three different heat inputs produced from CMT welding technique.

2. Materials and methods

2.1 Sample Preparation

The 316L ASS used in this study was 120 x 75 x 3 mm were prepared for various experiments utilizing an Electrical Discharge Machining (EDM). The samples were cut into precise dimensions for testing purposes. The welds were made using the cold metal transfer welding (CMT) process using an austenitic SS filler electrode 316L with different heat inputs. Argon was used as shielding gas and the flow rate was maintained at 10 liters per minute to ensure proper protection during welding. Table 1 represents the chemical composition of base metal (BM) and the welding electrode used during welding. Figure 1 shows the welded plates with different heat inputs.

In Table 2, the welding parameters for different heat input levels are presented. The heat inputs (HI) for each welding condition were calculated using equation (1).

$$HI = \eta \frac{V*I}{s} \text{ KJ/mm} \quad \ldots\ldots\ldots\ldots\ldots\ldots\ldots (1)$$

Where, I- welding current in amperes (A), s- welding speed in mm/s, V- voltage in volts (V), and η- efficiency of GTAW as 0.7 [15].

Table 1. Table represents the chemical composition of base metal and filler in wt%

Materials	C	Si	Mn	P	S	Cr	Mo	Ni	N	Co	Cu	Fe
AISI 316L ASS	0.020	0.450	1.39	0.031	0.003	16.936	2.272	10.054	0.002	-	-	Bal
ER 316L Filler	0.03	0.5	1.89	-	-	17.94	2.85	11.84	-	-	0.24	Bal

Table 2. Table represents the welding variables in differing welding currents

Specimens	Welding Speed (s) (mm/s)	Current (A)	Voltage (V)	Heat input (KJ/mm)
HHI	1.51	100	10	0.4634
MHI	1.79	110	10	0.4302
LHI	1.97	120	10	0.4264

2.2 Mechanical properties

Tensile tests were conducted on the welded samples with specific dimensions using a wire cut EDM machine. The samples had a length of 120 mm, width of 25 mm and gauge length of 30 mm. Tensile experiments were conducted on welded samples following the ASTM E8 standard with universal testing machine at a crosshead speed of 20 mm/min. This allowed for the evaluation of the mechanical properties of the welds. The results obtained from the tensile tests provided insights into the strength and ductility of the welded specimens. The data collected from the experiments enabled the analysis of the performance of the welds under tension [16].

3. Results and discussion

3.1 Tensile Test

Figure 1 illustrates the bar plot of ultimate tensile strength (UTS), yield strength (YS), and percentage elongation for the base metal (BM) and three welded samples (HHI, MHI and LHI). Three samples were tested under each condition and the average tensile strength of these three results was determined. 316L BM shows average UTS (608 MPa), YS (358 MPa) and higher % elongation (52%) compared to other welds due to the soft austenitic phase [17]. It was also found that the average UTS of the LHI sample (610 MPa) was higher compared to the MHI (603 MPa) and HHI (601 MPa). Due to the higher chromium and nickel contents in the weld metal, the YS of LHI was higher (375 MPa) than that of MHI (362 MPa) and HHI (359 MPa).

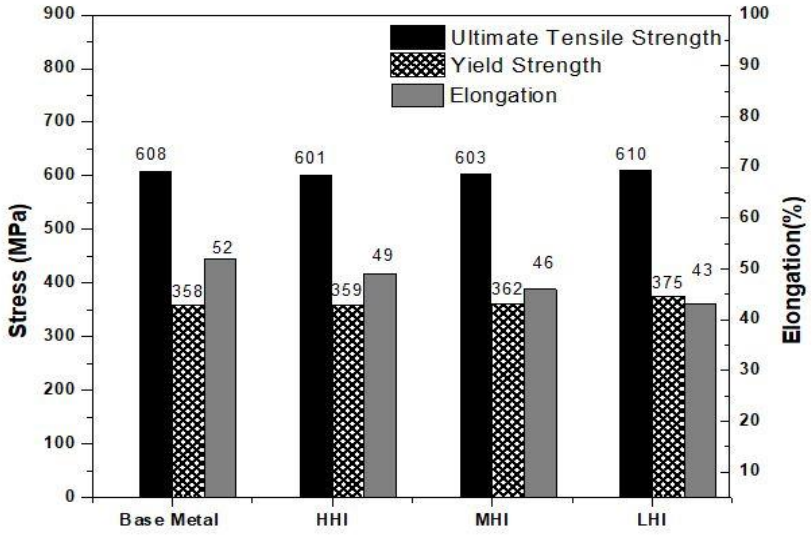

Figure 1. Ultimate Tensile Strength, Yield Strength and % Elongation of 316L BM, HHI, MHI and LHI weld specimen

3.2. ANSYS

ANSYS R18.1 is used to analyze the tensile specimen specified by ASTM E-8 standard. The welding is designed using design modeler in ANSYS as shown in Fig.2. The elemental mesh was created using elemental size 0.8 mm having minimum edge length 1 mm [18]. All elements exhibit a hexahedral shape. The 3D- Finite element model was created in ANSYS using 8-node three-dimensional Solid 185 elements. Static calculations of the welded joints were performed using the equivalent structural element Solid 185. After structural analysis, appropriate boundary conditions were applied. The total deformation and equivalent von Misses stress of the welded structure were calculated.

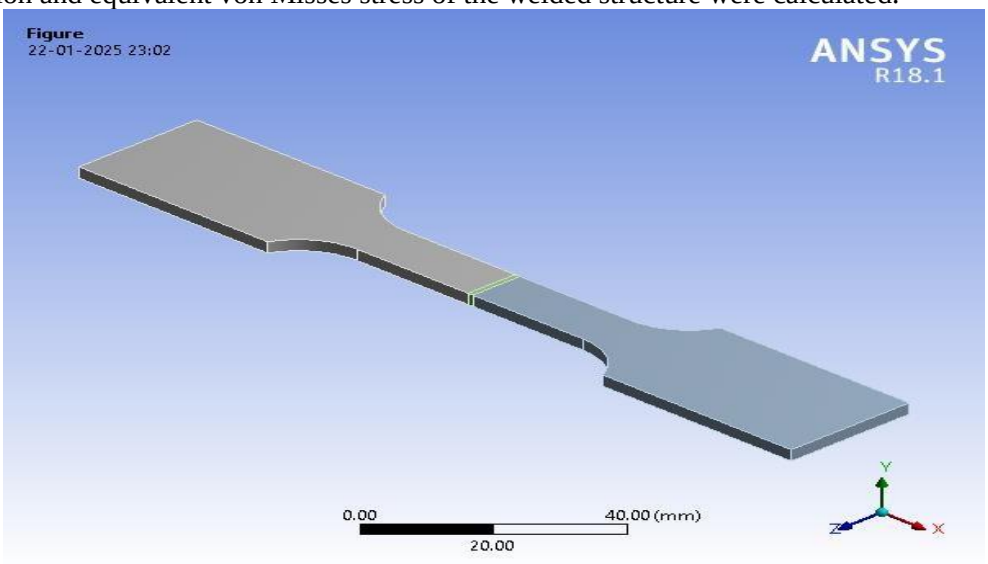

Figure 2. ANSYS geometry of the weldments.

3.2.1. Meshing

The adaptive size function having coarse relevance center with element size 0.80 mm were used [19]. The number of nodes created is 88232, number of elements taken 17906 and element quality 0.95 as shown in Fig.3. The smooth inflation progression, characterized by a transition ratio of 0.272 across five maximum steps, exhibits a growth rate of 1.2.

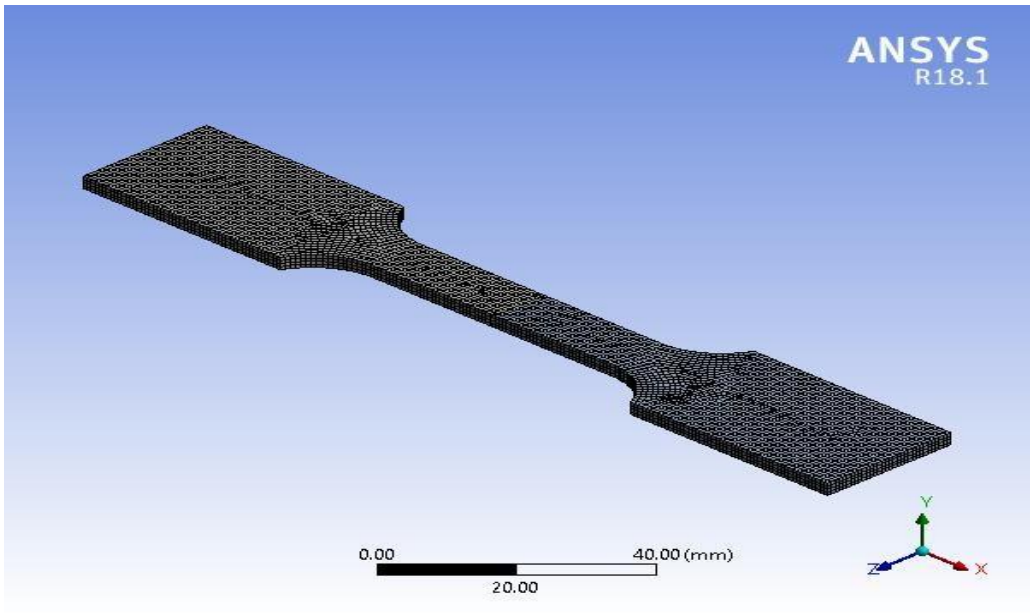

Figure 3. Meshing of the weldments

3.2.2. Boundary Condition

After structural analysis, weld metals were analyzed using boundary conditions as shown in fig.4. The linear format of the data used in ANSYS to simulate the welding process. The model is created due to the plate geometry's symmetrical properties.

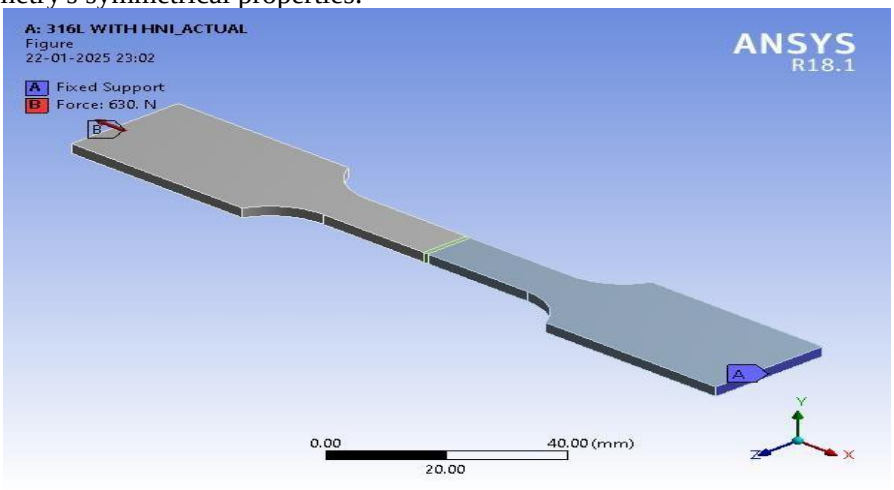

Figure 4. Applying Boundary Conditions

3.2.3. Displacement

In this study, finite element analysis was used to determine the maximum deformation under the applied load. The maximum deformation and minimum deformation occurred at top and bottom of the specimen. It was observed that HHI (31.98 mm) was highest as compared to MHI (30.01 mm) and LHI (28.52 mm) due to the high amount of composition of the alloying elements which is beneficial for deformation of the element [20]. Figure 5 (a) – (c) depicts the total deformation of the welded specimen.

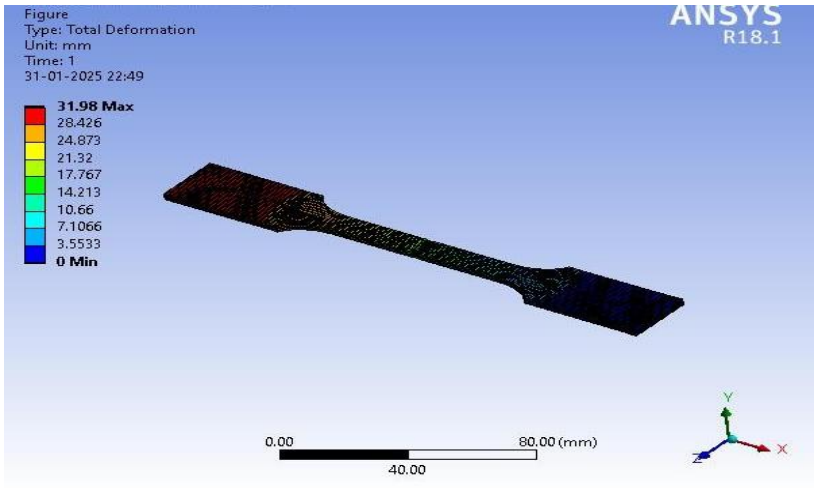

Figure 5 (a). Total deformation of HHI

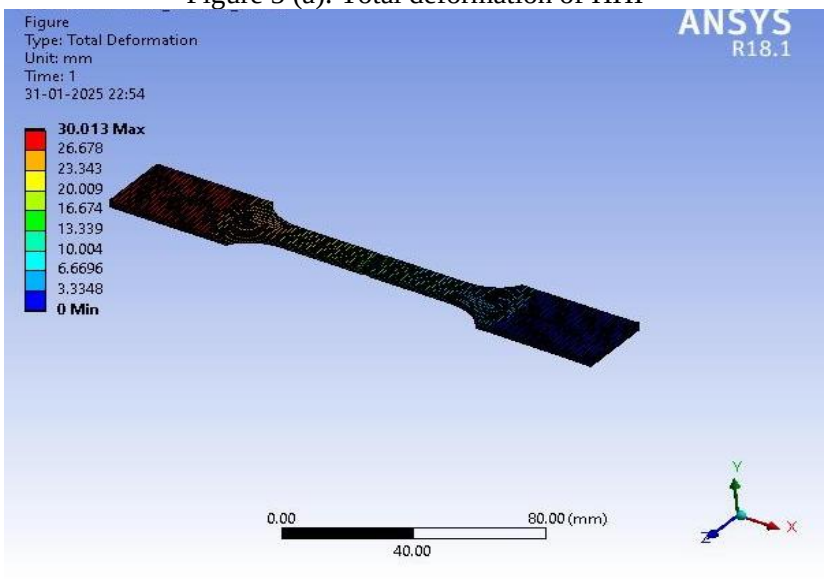

Figure 5 (b). Total deformation of MHI

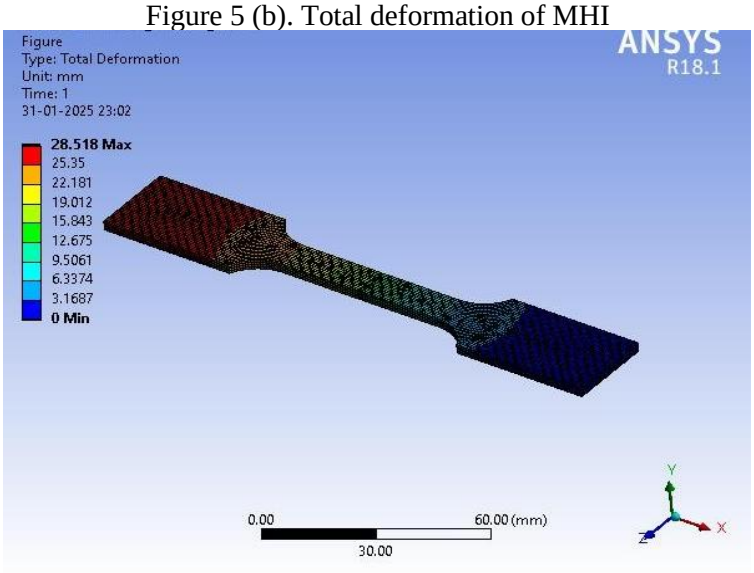

Figure 5 (c). Total deformation of LHI

3.5.5. Equivalent (Von-Mises) Stress of the weldments

The Equivalent (Von Mises) stresses were analysed using ANSYS R18.1. Figure 6 (a-c) shows the Von Mises Stress occurring at HHI, MHI and LHI weld. The Von Mises stress occurring at the weld joint is highest for LHI (376.8 MPa) as compared to MHI (366.52 MPa) and HHI (359.67 MPa) due to the input parameters such as high welding current (120A) and the heat input calculations from equation (1).

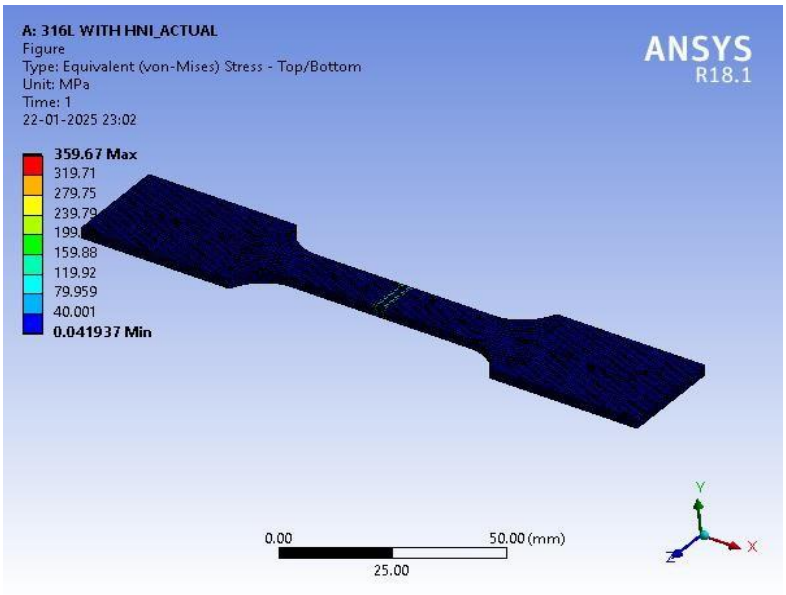

Figure 6 (a). Equivalent Von Mises stress of HHI

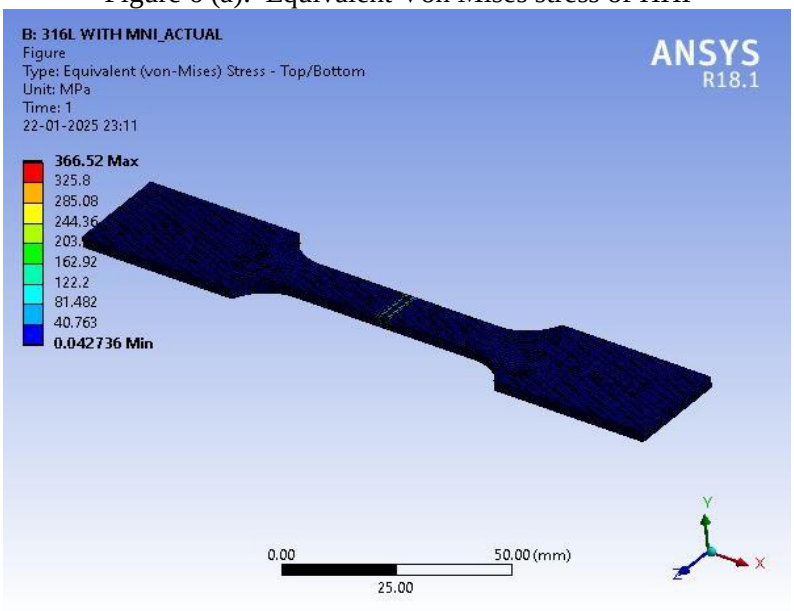

Figure 6 (b). Equivalent Von Mises stress of MHI

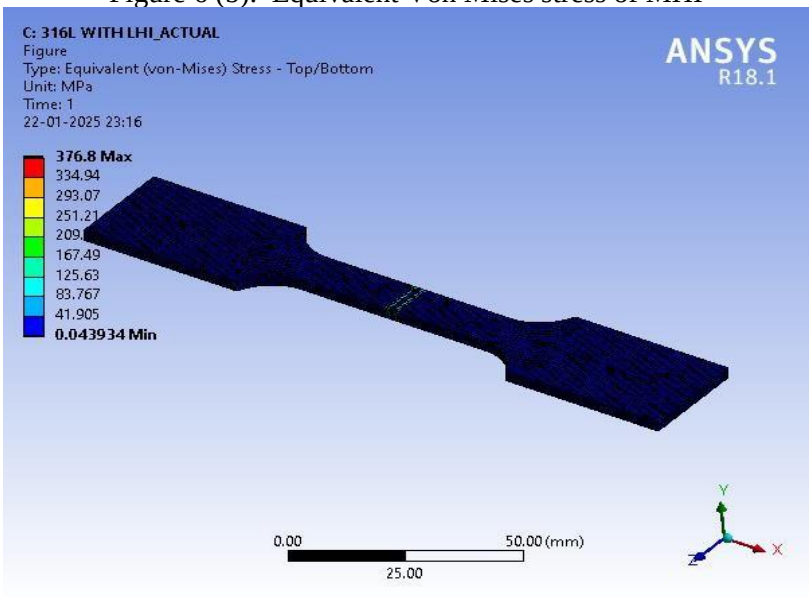

Figure 6 (c). Equivalent Von Mises stress of LHI

3.5.6 Comparison of experimental results with finite element models

Figure 7 represents the comparison of experimental results of yield strength occurring in HHI, MHI and LHI with Von Mises Stress occurring with ANSYS R18.1. The experimental results shows good agreement with simulation results obtained with finite element analysis. The Von Mises stress occurring at different weldments found to be highest as compared to experimental results obtained with tensile test. These results predict the yielding point of the material where Von Mises stress should be greater than the yield strength such that the yielding occurs [21].

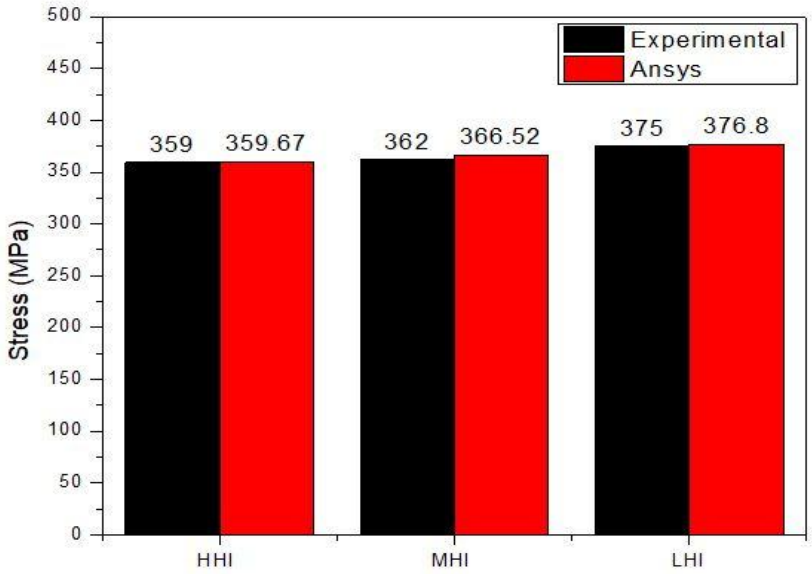

Figure 7. Comparison of Yield Strength with Von Mises Stress of HHI, MHI and LHI

4. Conclusions

In this study, 316L ASS welds were produced using CMT welding with different heat inputs. The mechanical properties of the weldments were examined and compared with simulation results using ASNSYS R18.1.

1. The tensile strength of LHI welds is the highest compared to MHI and HHI welds, which is due to the higher chromium and nickel content in the weld metal.
2. The total deformation of HHI welds based on ANSYS R18.1 was found to be greater than MHI and LHI welds due to the higher percentage of alloying elements in the welds.
3. The Von Misses stress for LHI weld was found to be highest compared to MHI and LHI weld due to the input parameters during welding.

Acknowledgements: The authors express their gratitude to the Director, VNIT, Nagpur for granting permission to conduct the experiments in the laboratories.

Conflict of Interests: The authors declare no conflict of interest.

References

[1] Hou, J. (2024) Microstructure Evolution and Performance of Additive Manufactured 316L Stainless Steel in High Temperature Nuclear Environment (Doctoral dissertation, The University of Manchester (United Kingdom)).

[2] Baldev, R., Kamachi Mudali, U., Vijayalakshmi, M., Mathew, M. D., Bhaduri, A. K., Chellapandi, & Venkatraman, B. (2013) Development of stainless steels in nuclear industry: with emphasis on sodium cooled fast spectrum reactors history, technology and foresight. AdvancedMaterialsResearch, 794, 3-25.

[3] Saha Podder, A., & Bhanja, A. (2013) Applications of stainless steel in automobile industry. Advanced Materials Research, 794, 731-740.

[4] Ishfaq, K., Anjum, I., Pruncu, C. I., Amjad, M., Kumar, M. S., & Maqsood, M. A. (2021) Progressing towards sustainable machining of steels: a detailed review. Materials, 14(18), 5162.

[5] Ahmad, A., Abdullah, S. R. S., Hasan, H. A., Othman, A. R., & Ismail, N. I. (2021) Aquaculture industry: Supply and demand, best practices, effluent and its current issues and treatment technology. Journal of Environmental Management, 287, 112271.

[6] Sverdrup, H. U., & Olafsdottir, A. H. (2019). Assessing the long-term global sustainability of the production and supply for stainless steel. BioPhysical Economics and Resource Quality, 4(2), 8.

[7] Vakili, M., Koutník, P., Kohout, J., & Gholami, Z. (2024) Analysis, Assessment, and Mitigation of Stress Corrosion Cracking in Austenitic Stainless Steels in the Oil and Gas Sector: A Review. Surfaces (2571-9637), 7(3).

[8] Tembhurkar, C., Kataria, R., Ambade, S. P., & Verma, J. (2022) A Critical Review on Dissimilar Joining of ASS and FSS. In Proceedings of the International Conference on Industrial and Manufacturing Systems (CIMS-2020) Optimization in Industrial and Manufacturing Systems and Applications (pp. 505-518). Springer International Publishing.

[9] Verma, J., & Taiwade, R. V. (2017) Effect of welding processes and conditions on the microstructure, mechanical properties and corrosion resistance of duplex stainless steel weldments—A review. Journal of Manufacturing Processes, 25, 134-152.

[10] Magudeeswaran, G., Balasubramanian, V., & Reddy, G. M. (2014). Effect of welding processes and consumables on fatigue crack growth behaviour of armour grade quenched and tempered steel joints. Defence Technology, 10(1), 47-59.

[11] Haq, A. U., Kavit, A. K., Rao, T., Buddi, T., Baloji, D., Satyanarayana, K., & Singh, S. K.(2019) Evaluation and optimization of material properties of ASS 316L at elevated temperatures using response surface methodology. Materials Today: Proceedings, 18, 4589-4597.

[12] Dharavath, B., Naik, M. T., Badrish, A., Buddi, T., & Saxena, K. K. (2023). Experimental and Finite Element Studies of Stretch Forming Process for ASS 316L at Elevated Temperature. Indian Journal of Engineering and Materials Sciences (IJEMS), 29(6), 744-749.

[13] Mani, C., Karthikeyan, R., Kannan, S., & Periasamy, C. (2020). Optimization of tensile properties of 316L stainless steel and Monel 400 weld joints using genetic algorithm. Materials Today: Proceedings, 27, 2846-2851.

[14] Ghumman, K. Z., Ali, S., Khan, N. B., Khan, M. I., Ali, H. T., & Ashurov, M. (2024). Optimization of TIG welding parameters for enhanced mechanical properties in AISI 316L stainless steel welds. The International Journal of Advanced Manufacturing Technology, 1-13.

[15] Tembhurkar, C., Kataria, R., Ambade, S., Verma, J., Sharma, A., & Sarkar, S. (2021). Effect of fillers and autogenous welding on dissimilar welded 316L austenitic and 430 ferritic stainless steels. Journal of Materials Engineering and Performance, 30, 1444-1453.

[16] Nurdin, H., Purwantono, P., & Umurani, K. (2021). Tensile strength of welded joints in low carbon steel using metal inert gas (MIG) welding. INVOTEK: Jurnal Inovasi Vokasional dan Teknologi, 21(3), 175-180.

[17] Lehmhus, D. (2024). Advances in Metal Casting technology: A Review of State of the Art, Challenges and Trends—Part II: Technologies New and Revived. Metals, 14(3), 334.

[18] Ambade, S., Kataria, R., Tembhurkar, C., & Meshram, D. (2023). Experimental and finite element analysis of temperature distribution in 409 M ferritic stainless steel by TIG, MIG and SMAW welding processes. Advances in Materials and Processing Technologies, 9(3), 843-858.

[19] Tavares, L. M., André, F. P., Potapov, A., & Maliska Jr, C. (2020). Adapting a breakage model to discrete elements using polyhedral particles. Powder Technology, 362, 208-220.

[20] Gowthaman, P. S., Jeyakumar, S., & Sarathchandra, D. T. (2024). Study on Heat Input Effect of 316L Stainless Steel Thin-Walled Parts Processed by Wire Arc Additive Manufacturing. Journal of Materials Engineering and Performance, 1-18.

[21] Donato, G. H., & Bianchi, M. (2011). Numerical modeling of uneven thermoplastic polymers behaviour using experimental stress-strain data and pressure dependent von Mises yield criteria to improve design practices. Procedia Engineering, 10, 1871-1876.